J Intell Robot Syst (2015) 77:73–93
DOI 10.1007/s10846-014-0098-6

Switched Control to Robot-Human Bilateral Interaction for Guiding People

Paulo Leica · Juan Marcos Toibero · Flavio Roberti · Ricardo Carelli

Received: 15 January 2014 / Accepted: 26 August 2014 / Published online: 9 September 2014

Abstract This paper presents a switched control strategy to interpret and design a human-robot bilateral interaction when a human follows a non-holonomic mobile robot at a desired distance while the robot is already following a known path. Furthermore, it proposes and experimentally validates a model that mathematically describes the human behavior when performing the specific task of tracking a mobile robot. This model is useful for the purposes of the control system design and its associated stability analysis. A switched system is proposed to model the complete human-robot behavior. The switching strategy is based on the human-robot relative position and on the human intention to follow the robot. Control errors are defined in terms of human to robot and robot to path instantaneous distances. Stability analyses for the individual controllers, as well as for the complete switching system, are provided by considering Lyapunov theory. Real human-robot interaction experiments show the good performance of the proposed control strategy.

Keywords Human-robot interaction · Bilateral interaction · Mobile robots · Lyapunov stability

P. Leica · J. M. Toibero · F. Roberti (✉) · R. Carelli
Instituto de Automática, Universidad Nacional de San Juan, Av. San Martin Oeste 1109, San Juan J5400ARL, Argentina
e-mail: froberti@inaut.unsj.edu.ar

P. Leica
e-mail: pleica@inaut.unsj.edu.ar

J. M. Toibero
e-mail: mtoibero@inaut.unsj.edu.ar

R. Carelli
e-mail: rcarelli@inaut.unsj.edu.ar

J. M. Toibero · F. Roberti · R. Carelli
Consejo Nacional de Investigación Científicas y Técnicas, San Juan, Argentina

1 Introduction

In recent years intensive work has been made with the aim of providing mobile robots the ability to move and interact with a high degree of autonomy in unstructured environments. In current robotic applications, these environments not only involve objects and other robots, but also raise awareness of the need to interact with humans. The usage of robots in human environments for service, people assistance, housework, etc., where the robots have to interact with humans, has been increasing in last years and it is expected that such robots become more common in the near future. Today, the challenge is to find safe interactions between robots and humans, where the robot interacts in a friendly and safe way with the human with or without physical contact. This latter approach is of interest in this work; where the robot can interpret human behavior and the person participates actively with the robot, through bilateral interactions. Human-robot interaction is said to be

bilateral when, during the task, both the behavior of the human can be changed by robot actions as well as the behavior of the robot can be changed by human decisions. Bilateral interactions are very important, for example, to guide people, where the robot should not only guide the person through an environment but also to interpret a certain level of human behavior, such as: difficulty walking (elderly or disabled persons), to interpret if the human wants to continue or not with the tour, the desired position of the human in the interaction, etc.

Some researchers have addressed these topics. Published papers considering this problem are, as e.g. the people tracking case presented in [1] and the monitoring of people in [2, 3]. In these cases, the human is the leader and the interaction is unilateral, the human is the only decision maker. An approach to locally optimize the work of cooperative robots and get the minimum displacement of human beings on a mission to guide people is also presented in [4]. This paper assumes the existence of a drag force that attracts the people behind the robot and the only goal of the leader robot is to reach the next point of the task. Whereas in [5] harmonic rules are proposed to ensure a smooth, safe navigation in a human-robot system. In this same paper, it is analyzed the interaction in such a way that people are considered as moving obstacles. There are also other proposals, for instance, the one in [6], where a guide robot moves around exhibitions guiding visitors. References [7, 8] report robots which are able to provide information to the user, the interaction with human is through facial expressions, gestures and body language. On the other hand, the increase in human-robot relations justifies the importance of studying the human behaviors in the robot-human interaction. Some research works consider this problem. One of the first projects related to modeling human behavior was done in [9], which describes quasi-linear analytical models for a human pilot. In [10] proposals have been offered to differentiate normal and suspicious behavior based on the trajectories described by humans. In [11] it is obtained a specific model for the gait of each person based on fuzzy finite state machines that can help in the diagnosis of walking disorders. In [12] it is derived a model for the personal gait of individuals based on neural networks. Furthermore, in [13] it is presented a differential system which accurately describes the geometry of locomotive trajectories of humans with non-holonomic constraint in the absence of obstacles. In [14] it is proposed a stable control scheme for bilateral teleoperation of mobile robots in the presence of obstacles with an approximated model of the human operator. In [15] a model that reproduces the movements of leg, foot and ankle during the human walking was proposed, taking into account the human anthropomorphic limitations. This work was subsequently extended to hands and thorax [16]. It therefore remains clear that modeling the human behavior is an area of current research within human-robot interaction.

This work proposes a switched control strategy for human-robot interaction in the task of a mobile robot guiding a human being along a desired path. Guiding a person at a desired distance is solved using bilateral interaction. The human-robot interaction considered in this work is said to be bilateral because the robot not only follows the desired path but also it has to interpret human intentions in order to modify its behavior during the task. In fact, the human may want to continue or not with the tour, or want to change his relative position while performing the task, either alongside or behind the robot. On the other hand, the human not only follows the robot but also he can make several decisions that affect the interaction. The major contributions of this paper are not only the proposal of novel robot controllers but also the model of the human behavior when executing the task. Moreover, the stability proof for all controllers and the stability proof of the complete switched system are also presented. Finally, the good performance of the proposed system is shown through experimental results.

The work is organized as follows. Section II describes the system and it presents the problem statement. Section III presents the control system design and the stability proof based on the Lyapunov theory. Section IV describes the full switching system. Section V presents and comments the experimental results. Finally, Section VI establishes the conclusions of the work.

2 System Description

2.1 Problem Statement

A novel control strategy is proposed for the bilateral interaction between a human being and a mobile robot. This control strategy makes the robot able to

guide a human while it follows a specified path. It is expected human and robot to maintain a desired distance between them, defined sometimes by the robot and sometimes by the human. This proposal includes the control laws needed to regulate the relative distance between the human and the robot. To accomplish this task, a path following control algorithm for the robot is firstly implemented, and secondly several control laws are proposed to control the robot-human distance. In the design of the control strategy, an interaction free zone and an interaction zone are defined by considering a minimum distance ρ_{min} and a maximum distance ρ_{max} around the robot. Additionally, Fig. 1a shows two different zones defined within the interaction zone: *Zone 1* (interaction) when the human is located behind the robot, *Zone 2* (interaction) when the human is located beside the robot, whereas a *Safety zone* (zone free of interaction) prevents physical contact between the robot and the human and it is bounded by ρ_{min}. When the human enters the interaction zone (*Zone 1* or *Zone 2*), the robot must achieve two joint objectives: to follow the specified path and to maintain a desired distance from the human. The only way for the robot to achieve both goals is by controlling the speed at which it travels over the path.

During the interaction task, the robot has to be able to interpret some human intentions:

i) If the human wants to interact with the robot or if he wants to leave the task. The robot will interpret that the human wants to follow it if he is inside the interaction zone and if the relative orientation between them is in the interval $(-\pi/2, \pi/2)$, according to the natural walking of human beings. On the other hand, the robot will interpret that the human wants to leave the task if he is outside the interaction zone or if the relative orientation between them is outside the interval $(-\pi/2, \pi/2)$.

ii) If the person wants to change the interaction zone (back↔beside). This human intention is detected based on the location of the human, i.e., if the human is inside *Zone 1* then the robot will interpret that he wants to follow it from behind, and if the human is inside *Zone 2* then the robot will interpret that he wants to follow the robot beside it.

iii) The speed at which the human wants to follow the robot. It is expected that the robot has the ability of guide a person while keeping the desired relative distance but navigating at the human desired speed.

Additionally, the robot has to be able to decide who (human or robot) is the responsible of regulate de relative distance between the human and the robot. For this purpose interaction sub-zones are defined, where the goal is that the human remains at the desired distance (dash line). Figure 1b shows that *Zone 1* is divided in two: *Zone 1H* where the human controls the interaction; and in the *Zone 1R* where the interaction is controlled by the robot (only in special cases, when the human speed is outside of the robot velocity limits, the interaction is controlled by the human as will be explained later). Similarly, Fig. 1c shows that *Zone 2* is divided in two: *Zone 2H* where the human controls the interaction and *Zone 2R* where the interaction

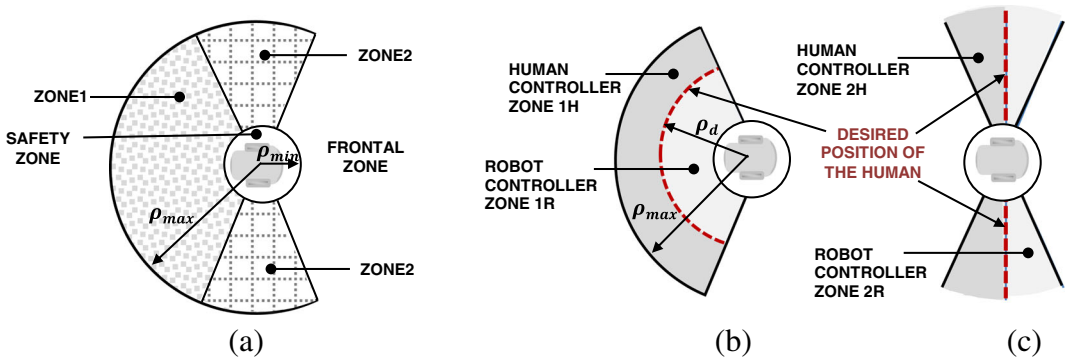

Fig. 1 **a** Robot-human system interaction zones **b** Robot-human system interaction zone 1 **c** Robot-human system interaction zone 2

is controlled by the robot (only in special cases, when the human speed is outside of the robot velocity limits, the interaction is controlled by the human as will be explained later).

3 Controllers Design

This section presents the design and stability analysis of the controllers that regulate the robot navigation in the different situations of the interaction task. These controllers will be later included in a switched control structure. It is also addressed in this section the human behavior modeling during the interaction task. With this aim, variation laws for the human angular and linear velocities (called *human controller* in this work) are proposed, considering that the natural human locomotion can be described as a non-holonomic kinematics [13, 18]. Then, a parametric identification and validation process is carried out for the proposed *human controller* with a set of 70 experiments performed by 7 different persons, taking into account the stereotyping and smoothness trajectories of people reported in the literature [19, 20]. Then the proposed *human controller* is simplified under some reasonable assumptions and validated again with the aim of performing the stability analysis of the system. It is important to note that, even when the human is obviously stable, a formal stability analysis of the *human controller* is important since it will be later included in the complete switched control system. Therefore, the stability properties of the *human controller* will be used in the stability analysis of the complete switched control system.

3.1 Path Following Controller for the Mobile Robot

The control objectives for the robot to follow a known path are: *i)* $\left\{\tilde{\psi}\right\} = 0$, where: $\tilde{\psi} = \psi_{Ro} - \psi_d$ and *ii)*: $\{d\} = 0$. This controller has been proposed and validated previously in [17], being defined by:

$$\begin{bmatrix} v_{Rc} \\ \omega_{Rc} \end{bmatrix} = J_1^{-1} \begin{bmatrix} v_d \cos\psi_d + k_{satx} \tanh\left(k_x \tilde{x}_R / k_{satx}\right) \\ v_d \sin\psi_d + k_{saty} tanh\left(k_y \tilde{y}_R / k_{saty}\right) \end{bmatrix}. \quad (1)$$

Figure 2 shows the involved variables of the path following controller, where: J_1 is the Jacobian of the robot defined in [17]; $\tilde{x}_R = x_d - x_R$ and $\tilde{y}_R = y_d - y_R$ are position errors; P is the set of points which define the desired path; $P_d = (x_d, y_d)$ is the point on the path which is closer to the robot; d is the distance between the robot and P_d; v_{Rc} and ω_{Rc} are the robot control actions of the lineal velocity and angular velocity respectively; ψ_{Ro} is the orientation of the robot on the path; and ψ_d is the desired orientation of the robot on the path defined by the tangent line to the path at P_d; v_d is the desired velocity for the path following task. The errors are proved to converge $\tilde{x}_R \to 0$ and $\tilde{y}_R \to 0$ asymptotically [17].

It is important to highlight that v_d is a free variable which can be considered both fixed and variable without affecting the control objective. Therefore, it will be used to regulate the robot-human distance by designing different control laws for this velocity, according to the human intentions.

3.2 Robot Distance Controller (Human into Zone 1R)

This section considers that the human is into *Zone 1R* and he has the intention to follow the robot from behind. Therefore, the human-robot distance controller is addressed by defining a variation law for the velocity v_d as a function of the relative posture between the human and the robot. As mentioned before, this velocity is a free variable in the path following controller, therefore it can be used for this second control objective, i.e., to achieve and to maintain the desired relative distance $\rho_d(t)$ between the human and the visual approach (in this case the robot, as Fig. 3 shows), to position the human at the desired position (marked with a dashed line) specifically to position the human over the target point (continuous circle). Additionally, Fig. 3 shows the visual approach (dashed circle), which is his visual reference when walking behind the robot.

Figure 3 also shows the mobile robot and the human along with the involved variables. Note that the relative distance error between them is $\tilde{\rho}(t) = \rho_d(t) - \rho(t)$, being $\tilde{\rho}(t)$ the distance error, ρ is the distance between the robot and the human and $\rho_d(t)$ the desired distance, which are projected on the reference line; $v_H(t)$ and $\omega_H(t)$ are the linear and angular velocity of the human; $\psi_R(t)$ is the robot orientation to the reference line (Notice the difference between $\psi_R(t)$ and ψ_{Ro});$\psi_H(t)$ is the human orientation with respect to the line segment $\rho(t)$.$\tilde{\psi}_H(t) = \psi_H(t)$ because

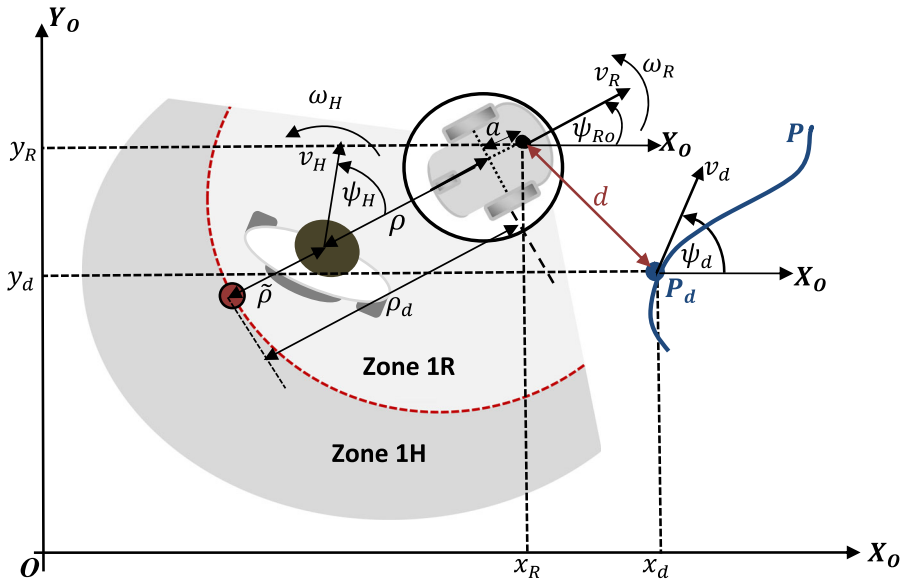

Fig. 2 Robot and the path in the reference **O**

$\psi_{Hd}(t) = 0$. This way, time derivative of distance error $\tilde{\rho}$(t) is:

$$\dot{\tilde{\rho}} = v_H(t)\cos\psi_H(t) - v_R(t)\cos\psi_R(t)\,. \tag{2}$$

Now, the control objective is that the relative distance between the robot and the human achieves the desired value, i.e., $\tilde{\rho}(t) = 0$. With this aim, the proposed control law is:

$$v_d = \frac{v_H(t)\cos\psi_H(t) + k_{sat\rho}\tanh\left(k_\rho\tilde{\rho}(t)/k_{sat\rho}\right)}{\cos\psi_R(t)}, \tag{3}$$

where $k_{sat\rho}$ and k_ρ are positive constants.

Theorem 1 *Let us consider the time evolution of the relative distance error between the robot and the human (2) and the proposed control law (3), and assume that the human has the intention of interact with the robot (human inside Zone 1R and* $|\psi_H(t)| < \pi/2$*); and assume also perfect velocity tracking, i.e.* $v_R(t) \equiv v_d$*. Then,* $\tilde{\rho}(t) \to 0$ *with* $t \to \infty$*.*

Proof By considering the hypothesis of perfect velocity tracking, i.e. $v_R(t) \equiv v_d$, (3) be substituted in Eq. 2 to obtain the following closed loop system:

$$\dot{\tilde{\rho}}(t) = -k_{sat\rho}\tanh\left(k_\rho\tilde{\rho}(t)/k_{sat\rho}\right).$$

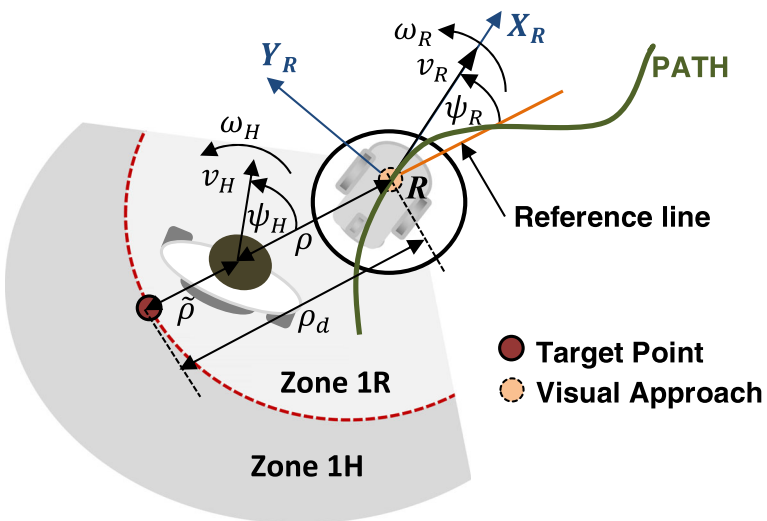

Fig. 3 Human-Robot reference system when the human is located Zone 1R

Now, for the stability analysis, the following Lyapunov candidate function is proposed $V = \tilde{\rho}(t)^2/2$, whose time derivative in system trajectories is:

$$\dot{V} = \tilde{\rho}(t)\dot{\tilde{\rho}}(t) = -\tilde{\rho}(t)k_{sat\rho}\tanh\left(k_\rho \bullet \tilde{\rho}(t)/k_{sat\rho}\right) < 0.$$

Then, $\tilde{\rho}\,(t) \to 0$ with $t \to \infty$.

Now, from (3), v_d could take values below zero making the robot going back on the path, or it could also take values above a maximum velocity or below a minimum velocity considered as a safe velocity. These situations are undesirable, so it is imposed the following condition on v_d:

$$0 < v_{Rmin} < v_d < v_{Rmax}. \tag{4}$$

Therefore, if condition (4) is not fulfilled, the responsibility of controlling distance ρ falls on the human. These situations are addressed in the following sections. □

3.3 Human Distance Controller (Human into Zone 1H)

This section addresses the human behavior modeling, when it has the intention of interact with a mobile robot in the specific considered task. This human behavior will be modeled as two non-linear equations which regulate the linear and angular velocities in the human movements, i.e. a structure for the *human controller* is proposed and then a parametric identification is performed. It is important to remark that this work does not consider the complexity of biomechanical system modeling of the human body but it is based on the observation of the human locomotion trajectories geometry and both the position and orientation of the human body along these trajectories. Important conclusions are reported in the literature about the stereotyping and smoothness trajectories [19, 20] of the natural human gait supporting the assumption of a non-holonomic behavior [13, 18]. Additionally, taking into account the purposes of the proposed human behavior model, it is considered that an adequately validated model under mentioned assumptions is suitable for this work. Finally, a stability analysis of the proposed *human controller* is made based on Lyapunov theory.

In order to find a nonlinear kinematic controller that models the human behavior, it is assumed that: i) the person has the intention intends to follow the robot at a desired known distance, ii) the human locomotion is modeled including a non-holonomic constraint [18, 19]: the human has no lateral movements, which in fact corresponds to natural human walking. Now, the goal is that the human controls the distance error $\tilde{\rho}$ and the orientation ψ_H (Fig. 4). The kinematics of the interaction between the human and the robot is defined by:

$$\begin{bmatrix} \dot{\tilde{\rho}}_H\,(t) \\ \dot{\psi}_H\,(t) \end{bmatrix} = \begin{bmatrix} v_H(t)\cos\psi_R(t) - v_R(t)\cos\psi_R(t) \\ \omega_H(t) + \frac{v_H(t)\sin\psi_H(t) + v_R(t)\sin\psi_{R(t)}}{\rho(t)} \end{bmatrix}. \tag{5}$$

It is proposed that the human behaves as described by:

$$\begin{bmatrix} v_H\,(t) \\ \omega_H\,(t) \end{bmatrix} = \begin{bmatrix} \frac{v_R(t)\cos\psi_R(t) - k_\rho\tilde{\rho}(t)}{\cos\psi_H(t)} \\ \frac{-v_H(t)\sin\psi_H(t) - v_R(t)\sin\psi_{R(t)}}{\rho(t)} - k_\omega\psi_H\,(t) \end{bmatrix} \tag{6}$$

Equation 6 has a conceptual interpretation, it can be seen that the controller reflects a human intuitive behavior when following the robot by adjusting the linear speed proportionally to the distance error and adjusting its angular velocity proportionally to the orientation error. Note that when $\psi_H = \pi/2$ the human has no intention to follow the robot, for this reason this situation is not considered in the analysis. Constants k_ρ and k_ω act as controller gains and they must be properly identify through a parametric identification process. It is expected that constants k_ρ and k_ω may vary from one person to other person, this parameters variation can be represented by $\Delta\delta_{k_\rho}$ and by $\Delta\delta_{k_\omega}$ respectively. In order to get a more accurately representation of the human behavior, it is considered the reaction time τ with $t^* = t - \tau$. Taking into account these parameters variation for each person and the time delay τ, then (6) can be rewritten as:

$$\begin{bmatrix} v_H\,(t) \\ \omega_H\,(t) \end{bmatrix} = \begin{bmatrix} \frac{v_R(t^*)\cos\psi_R(t^*) - \hat{k}_\rho\tilde{\rho}(t^*)}{\cos\psi_H(t^*)} \\ \frac{-v_H(t)\sin\psi_H(t^*) - v_R(t^*)\sin\psi_R(t^*)}{\rho(t^*)} - \hat{k}_\omega\psi_H\,(t^*) \end{bmatrix} \tag{7}$$

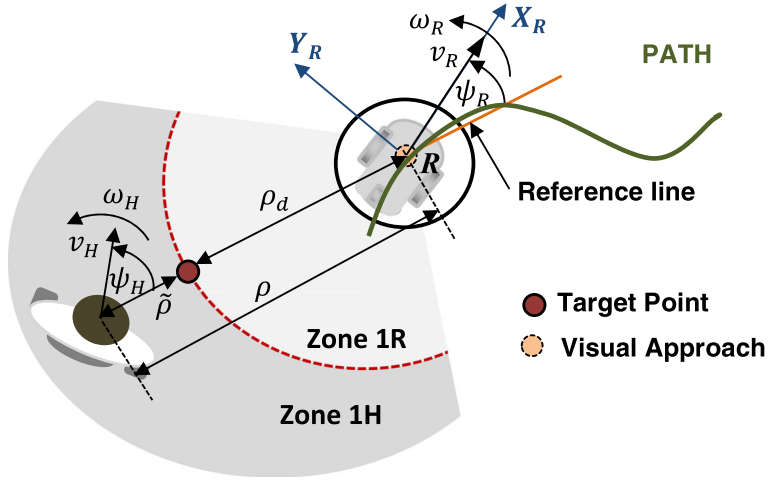

Fig. 4 Human-Robot reference system when the human is located Zone 1H

where $\hat{k}_\rho = k_\rho + \Delta\delta_{k_\rho}$ and $\hat{k}_\omega = k_\omega + \Delta\delta_{k_\omega}$. Substituting (7) in Eq. 5, the closed-loop equation for $\tilde{\rho}$ is obtained as:

$$\dot{\tilde{\rho}}(t) = -\hat{k}_\rho \tilde{\rho}(t^*) \frac{\cos\psi_H(t)}{\cos\psi_H(t^*)} - v_R \cos\psi_R(t) + \frac{v_R(t^*)\cos\psi_R(t^*)\cos\psi_H(t)}{\cos\psi_H(t^*)}$$

Defining $\alpha(t) = v_R \cos\psi_R(t)$ and $\gamma(t) = \cos\psi_H(t)$, the following expression is obtained:

$$\dot{\tilde{\rho}}(t) = -\hat{k}_\rho \tilde{\rho}(t^*) \frac{\gamma(t)}{\gamma(t^*)} + \left(\alpha(t^*)\frac{\gamma(t)}{\gamma(t^*)} - \alpha(t)\right) \tag{8}$$

Now, for the angular variable ψ_H:

$$\dot{\psi}_H(t) = -\hat{k}_\omega \psi_H(t^*) + v_H(t)\left(\frac{\sin\psi_H(t)}{\rho(t)} - \frac{\sin\psi_H(t^*)}{\rho(t^*)}\right) + \left(\frac{v_R(t)\sin\psi_R(t)}{\rho(t)} - \frac{v_R(t^*)\sin\psi_R(t^*)}{\rho(t^*)}\right)$$

Taking $\phi(t) = \sin\psi_H(t)/\rho(t)$ and $\beta(t) = v_R(t)\sin\psi_R(t)/\rho(t)$ then:

$$\dot{\psi}_H(t) = -\hat{k}_\omega \psi_H(t^*) + v_H(t)\left[\phi(t) - \phi(t^*)\right] + \left[\beta(t) - \beta(t^*)\right] \tag{9}$$

For the parametric identification of the *human controller* (6), 70 experiments were conducted with 7

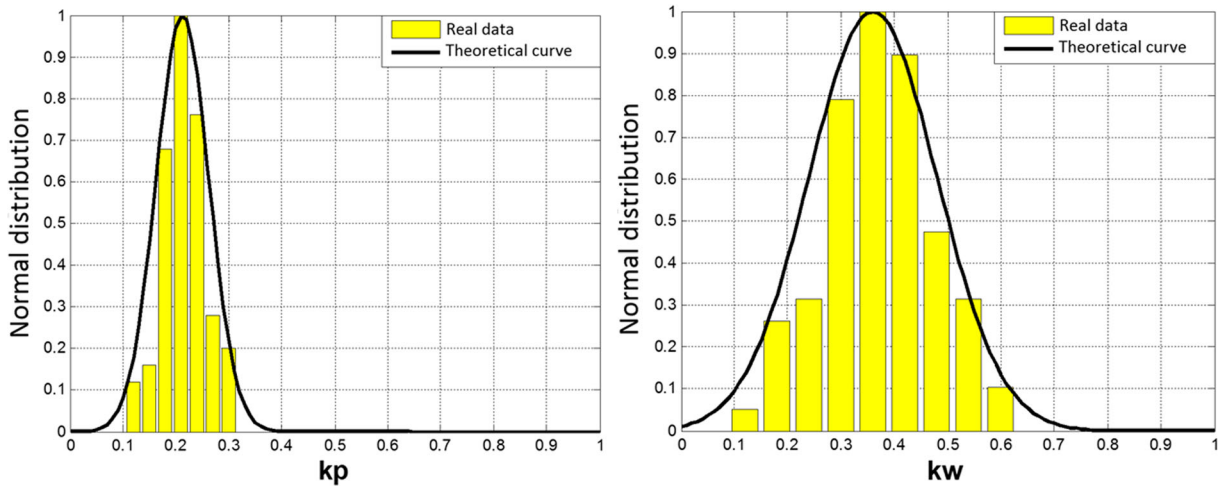

Fig. 5 Verification of the normal distribution nature of the experimental data

different persons, 5 men and 2 women between 25 and 40 years old. It is important to remark that selected persons have to be able to walk, and for the identification purposes they have to be able to walk at a speed above $0.3m/s$. Each person did 10 experiments without any previous training in using the proposed robotic system. Persons started from position (0,-2m), and they were asked to follow the robot at a desired distance of 1 meter, always oriented to the robot direction. No specific instructions were given to persons about the walking speed. The robot started from position (0,0) and traveled along a sinusoidal path with amplitude $1.5m$ and frequency $0.03\text{rad}/s$ at a lineal velocity of $0.3m/s$. Human variables (distance, position, orientation and linear velocity) were obtained through a leg detection algorithm, an α-β-γ filter and a laser rage sensor. These variables were calculated for each experiment with a sampling period of $ts = 0.1s$. The parameters k_ρ and $k_\omega$and values $\Delta\delta_{k_\rho}$ and $\Delta\delta_{k_\omega}$ were identified by a recursive least squares algorithm. On the other hand, the human reaction time τ was obtained from the analysis of the experimental curves. It was verified that the dataset of each identified parameter approximates a Gaussian distribution (Fig. 5), therefore some specific statistical tools were used to obtain the final values. The average values of the parameters for the 70 experiments are: $k_\rho = 0.2307$; $k_\omega = 0.3859$; $\Delta\delta_{k_\rho} = 0.051$; $\Delta\delta_{k_\omega} = 0.115$ and human average reaction time $\tau = 0.9s$

The resulting experimental curves and the proposed *human controller* are shown in Fig. 6 (distance error) and Fig. 7 (orientation error). Figures. 6 and 7 show the variance in the human behavior (solid lines) and the proposed *human controller* (dash line) for the distance error $\tilde{\rho}$ and the orientation error ψ_H respectively. Figures. 6 and 7 show that the human experimental curves correspond to the proposed controller, thus validating equations 8 and 9.

Now, in order to simplify these expressions, it is assumed a slow dynamics in the human behavior. That is, the human does not produce abrupt changes in position or orientation during the interaction task, and then the following conditions are approximately verified: $\left[\alpha(t) - \alpha(t^*)\right] \cong \varepsilon_\alpha$; $[\phi(t) - \phi(t^*)] \cong \varepsilon_\phi$; $[\beta(t) - \beta(t^*)] \cong \varepsilon_\beta$; $\gamma(t)/\gamma(t^*) \cong 1$. Here $\varepsilon_\alpha \varepsilon_\phi$ and ε_β are very small values, therefore Eqs. 8 and 9 can be rewritten as:

$$\begin{bmatrix} \dot{\tilde{\rho}}(t) \\ \dot{\psi}_H(t) \end{bmatrix} \cong \begin{bmatrix} -\hat{k}_\rho \tilde{\rho}(t^*) + \varepsilon_\alpha \\ -\hat{k}_\omega \psi_H(t^*) + \varepsilon_\phi \nu_H(t) + \varepsilon_\beta \end{bmatrix}$$

$$\begin{bmatrix} \dot{\tilde{\rho}}(t) \\ \dot{\psi}_H(t) \end{bmatrix} \cong \begin{bmatrix} -\hat{k}_\rho \tilde{\rho}(t^*) \\ -\hat{k}_\omega \psi_H(t^*) \end{bmatrix} \quad (10)$$

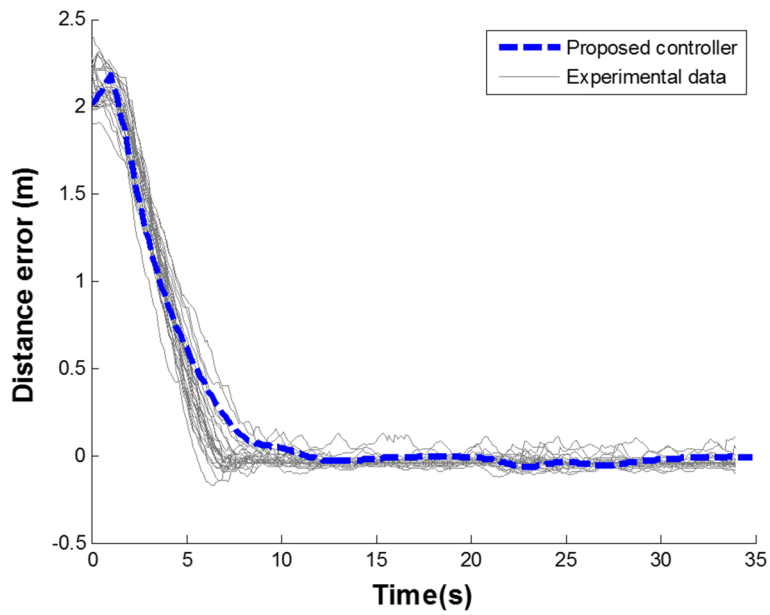

Fig. 6 Experimental distances error (Humans) and the proposed controller

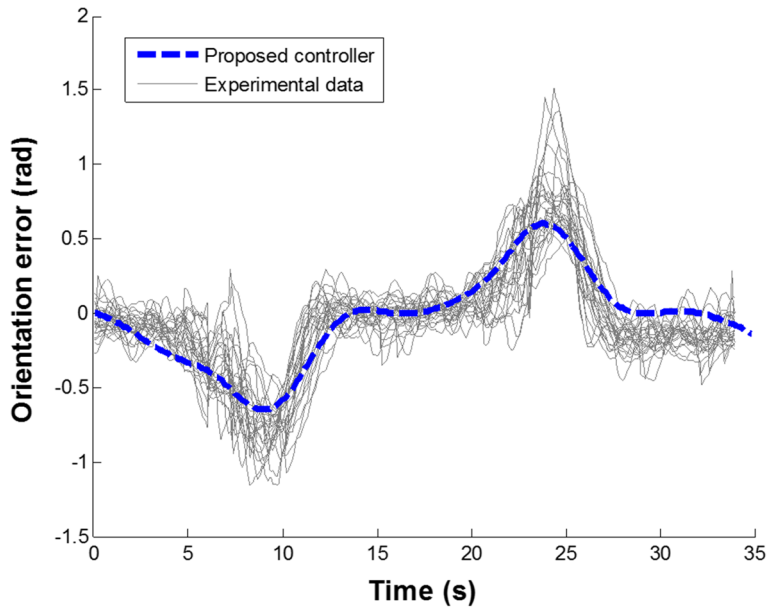

Fig. 7 Experimental orientation error (Humans) and the proposed controller

With this simplification, the *human controller* is:

$$\begin{bmatrix} v_H\ (t) \\ \omega_H\ (t) \end{bmatrix} = \begin{bmatrix} \frac{v_R(t)\cos\psi_R(t) - \hat{k}_\rho \tilde{\rho}(t^*)}{\cos\psi_H(t)} \\ \frac{-v_H(t)\sin\psi_H(t) - v_R(t)\sin\psi_R(t)}{\rho(t)} - \hat{k}_\omega \psi_H\ (t^*) \end{bmatrix} \tag{11}$$

A comparison was made between the human experimental curves and the errors evolution obtained with both Eqs. 8–9 and 10 to validate the simplified model (11). In figures 8 and 9 the simplified controller was represented with a solid line for $\tilde{\rho}$ and ψ_H respectively. It becomes clear that the simplified controller follows very closely the human behavior, thus validating the proposed controller in Eq. 11.

Once the proposed *human controller* is validated, it follows its stability analysis.

Theorem 2 *Let us consider the kinematic model of the interaction between the human and the robot* (5) *and the proposed simplified human controller* (11)*, and assume that the human has the intention of*

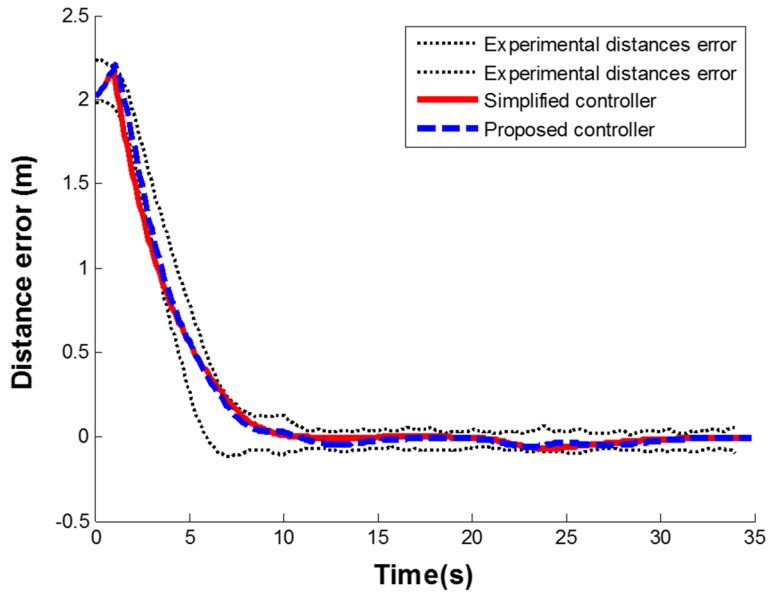

Fig. 8 Experimental distances error (standard deviation) and the ones for the proposed and simplified controller

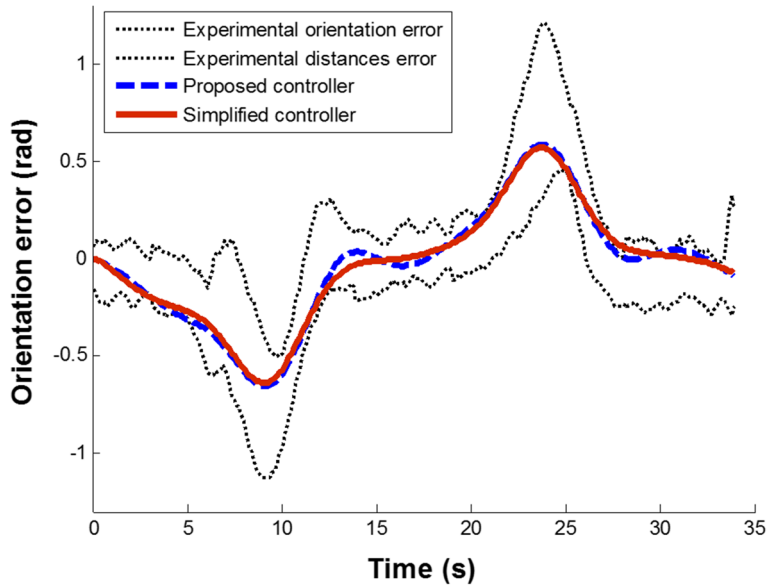

Fig. 9 Experimental orientation error (standard deviation) and the ones for the proposed and simplified controller

interact with the robot (human inside Zone 1H and $|\psi_H(t)| < \pi/2$*). Then,* $\tilde{\rho} \to 0 and \psi_H \to 0$ *with* $t \to \infty$.

Proof Substituting (11) in Eq. 5, the closed loop system equation (10) is obtained. According to [22] a system with delay can be expressed as:

$$\dot{x}_i(t) = -a_i x_i(t) - b_i x_i(t-\tau) \tag{12}$$

where a_i and b_i are system parameters. Comparing (12) with Eq. 10, $a_i = 0$, then the system is defined by:

$$\dot{x}_i(t) = -b_i x_i(t-\tau) \tag{13}$$

Using a transformation according to [19], (13) can be rewritten as:

$$\dot{x}_i(t) = -b_i x_i(t) + b_i^2 \int_{-2\tau}^{-\tau} x_i(t+\theta)\, d\theta \tag{14}$$

where θ represents an integration auxiliary variable. Rewriting (10) as Eq. 14:

$$\begin{bmatrix} \dot{\tilde{\rho}}(t) \\ \dot{\psi}_H(t) \end{bmatrix} = \begin{bmatrix} -b_1\tilde{\rho}(t) + b_1^2 \int_{-2\tau}^{-\tau} \tilde{\rho}(t+\theta)\, d\theta \\ -b_2\psi_H(t) + b_2^2 \int_{-2\tau}^{-\tau} \psi_H(t+\theta)\, d\theta \end{bmatrix} \tag{15}$$

where $b_1 = \left(k_\rho + \Delta\delta_{k_\rho}\right)$ and $b_2 = \left(k_\omega + \Delta\delta_{k_\omega}\right)$ are parameters of the human previously identify. For the stability analysis, the following Lyapunov candidate function is proposed:

$$V_1(x_1(t)) = \tilde{\rho}(t)^2/2 V_2(x_2(t)) = \psi_H(t)^2/2. \tag{16}$$

Considering the $i-$th Lyapunov candidate function and its time derivative in the trajectories of the system:

$$\dot{V}_i(x_i(t)) = x_i(t)\,\dot{x}_i(t) \tag{17}$$

Replacing (14) into Eq. 17:

$$\dot{V}_i(x_i(t)) = -b_i x_i(t)^2 + b_i^2 x_i(t) \int_{-2\tau}^{-\tau} x_i(t+\theta)\, d\theta \tag{18}$$

Now, the following design condition is proposed:

$$V_i(x_i(\xi)) < q_i^2 V_i(x_i(t)) \tag{19}$$

where V_i is the i-th Lyapunov candidate function; x_i is the i-th state; and $q_i > 1$. Considering $V_i(x_i(t)) = x_i(t)^2/2$ and $V_i(x_i(\xi)) = x_i(\xi)^2/2$ in Eq. 19:

$$x_i(\xi) < q_i x_i(t) \tag{20}$$

then:

$$\int_{-2\tau}^{-\tau} x_i(t+\theta) d\theta \cong x_i(\xi) < \tau q_i x_i(t) \tag{21}$$

Replacing (21) in Eq. 18:

$$\dot{V}_i\left(x_i(t)\right) < -b_i x_i\,(t)^2\left(1-\tau b_i q_i\right) \tag{22}$$

For the system to be asymptotically stable $\left(\dot{V}_i\left(x_i(t)\right) < 0\right)$ it should be met that: $\tau b_i < 1/q_i$ (since $b_i > 0$) Recalling that values obtained in the parametric identification are $b_1 = 0.2307 \pm 0.051$, $b_2 = 0.3859 \pm 0.115$ and $\tau = 0.9s$ then $q_{1min} = 3.944$ and $q_{2min} = 2.218$ fulfilling the design condition $q_i > 1$. Therefore the human proposed controller gives an asymptotically stable control system. □

Note that even when the human is obviously stable, this analysis finds relevance in the stability analysis of the overall switched system, which involves the control algorithms for the robot

3.4 Robot Distance Controller (Human into Zone 2R)

Note the difference between d_y and $\tilde{\rho}_y$, where d_y is the distance between the robot and target point, and $\tilde{\rho}_y$ is the distance between the human and target point, d_H is the distance between the human and the robot. As stated in previous sections, the human can decide the location to follow the robot. If he is inside *Zone2R*, then the robot will interpret that the human wants to follow the robot beside it. Figure 10 depicts this situation. In this context, the robot is unable to regulate distance $\tilde{\rho}_y$ while it follows the desired path. Therefore, the control objective for the robot, as well as the path following objective, is that $\tilde{\rho}_x \to 0$. The human will be in charge of regulating the value of $\tilde{\rho}_y$ and the target point can be located any value between $\rho_{min} < d_y < \rho_{max}$. Once again, the robot can regulate $\tilde{\rho}_x$ while following the desired path by handling v_d. It is important to note that in this case, the visual focus point (dash line circle in Fig. 10) is in front of the target point since the human follows the robot beside it but looking forward, which is natural in human gait. Now, by considering the time derivative of $\tilde{\rho}_x$:

$$\dot{\tilde{\rho}}_x = v_R - v_H \cos\psi_H \tag{23}$$

the following control law is proposed:

$$v_d = v_H \cos\psi_H - k_{satL\rho}\tanh\left(k_{L\rho}\tilde{\rho}_x / k_{satL\rho}\right) \tag{24}$$

where v_d is the robot velocity to achieve the control objective and where $k_{satL\rho}$ and $k_{L\rho}$ are positive constants, defined taking into account the maximum velocity of the robot.

Theorem 3 *Let us consider the time evolution of the relative distance error between the robot and the human* (23) *and the proposed control law* (24)*, and assume that the human has the intention of interact with the robot (human inside Zone 2R) and assume also perfect velocity tracking, i.e.* $v_R(t) \equiv v_d$. *Then,* $\tilde{\rho}_x\,(t) \to 0$ *with* $t \to \infty$.

Proof By considering the hypothesis of perfect velocity tracking, i.e. $v_R(t) \equiv v_d$, (24) can be substituted in Eq. 23 to obtain the following closed loop system:

$$\dot{\tilde{\rho}}_x = -k_{satL\rho}\tanh\left(k_{L\rho}\tilde{\rho}_x / k_{satL\rho}\right) \tag{25}$$

The following Lyapunov candidate function is proposed $V = \tilde{\rho}_x^2/2$, whose time derivative in system trajectories is:

$$\dot{V} = \tilde{\rho}_x\dot{\tilde{\rho}}_x = -\tilde{\rho}_x k_{satL\rho}\tanh\left(k_{L\rho}\tilde{\rho}_x / k_{satL\rho}\right) < 0.$$

Thus $\tilde{\rho}_x \to 0$ asymptotically, meaning that control objective is achieved. Therefore, it has been proved that the robot is able to regulate the distance $\tilde{\rho}_x$ while following the desired path. □

Similar to Section III.B, if condition (4) is not fulfilled, the responsibility of controlling distance $\tilde{\rho}_x$ falls on the human.

3.5 Human Distance Controller (Human into Zone 2H)

In this case, the human decides to follow the robot beside it and the robot will navigate following the desired path with the human velocity (Fig. 11). Therefore the human will be not only responsible for deciding the value of $\tilde{\rho}_x$ but also he will be responsible for regulating $\tilde{\rho}_y$ and ψ_H. If the human is located within the interaction zone, d_y can take values between $\rho_{min} < d_y < \rho_{max}$. The behavior of the human being in this task is modeled by the same controller explained in Section III.C. This model is valid since the visual reference point is located in front of the target point instead of being over the robot. This assumption is according to the non-holonomic natural walking of humans. Once, the controllers stability has been verified, the effect of the switching will be next studied.

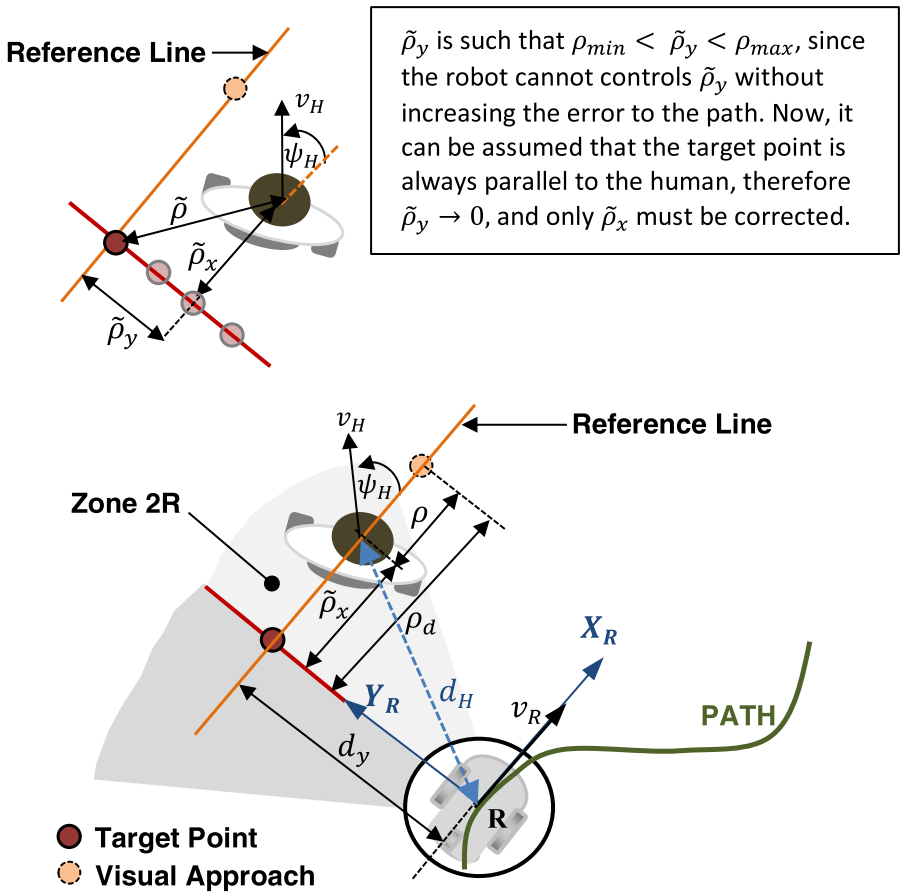

Fig. 10 Human-Robot reference system when the human is located in the zone 2R

4 Switching System

This section formalizes the proposal of modeling the bilateral human-robot interaction by a switching system of the previous controllers, and the stability analysis of the whole system. A piecewise continuous switching signal $\sigma_A = i (i = 0, 1, 2, 3)$ is employed to describe the switching system by indicating the active controller at every instant as shown in Fig. 12.

The switching signal $\sigma_A = 0$ when the distance control is performed by the human and the robot travels the path at the constant velocity v_{Rmin}; $\sigma_A = 1$ when the distance control is performed by the human and the robot moves over the path at maximum velocity v_{Rmax}; $\sigma_A = 2$ when the distance control is performed by the robot (distance control 1: human behind the robot) and the human only controls its orientation. Finally, $\sigma_A = 3$ when the control distance is performed by the robot (control distance 2: human beside the robot) and the human controls its orientation. This way it is possible to switch between controllers by selecting the proper σ_A value. In this work this selection is the output of a logic-based supervisor whose entries are the human position with respect to the robot and the human velocity (as shown in Table 1). Some special cases will be analyzed later in the text.

It is a well-known fact that asymptotic stability (AS) of the individual controllers is not a sufficient condition for the stability of the switched system [22]. In order to be able to conclude about the overall switched system stability, it is required to analyze the switching effect over each one of the states of interest [23–26].

4.1 Stability Analysis of Human-Robot Switching: Human located behind the Robot

Switching will occur when the human passes from *Zone 1H* to *Zone 1R* or vice versa. Additionally, this

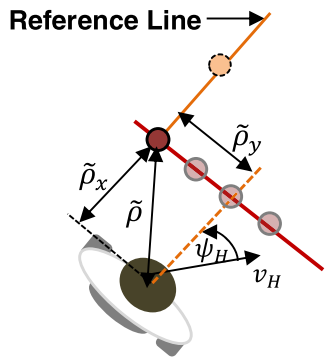

Analogously: $\tilde{\rho}_y$ is such that $\rho_{min} < \tilde{\rho}_y < \rho_{max}$, since the robot cannot control $\tilde{\rho}_y$ without moving away from the path. By assuming that the target point is always parallel to the human, it follows that $\tilde{\rho}_y \to 0$, and only $\tilde{\rho}_x$ must be controlled.

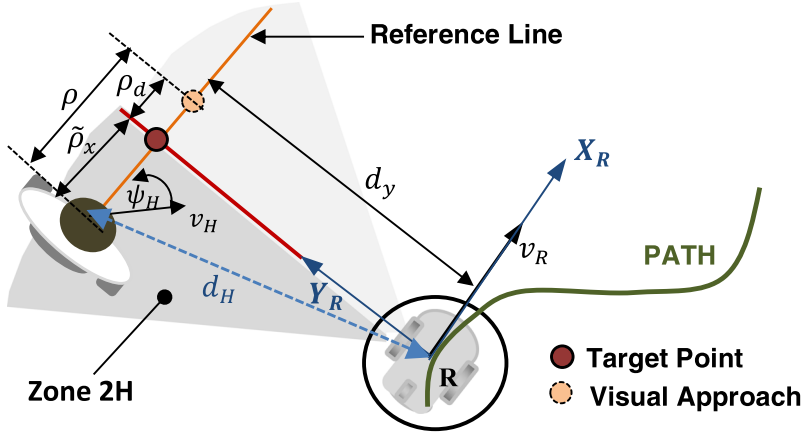

Fig. 11 Human-Robot reference system when the human is located in the zone 2H

same switching will occur when the human velocity overpasses the maximum value set for the robot velocity or the human velocity is less than v_{Rmin} (*Zone 1R* or *Zone 2R*) The robot will always be following the path. For this reason: d (distance to the path) and $\tilde{\psi}$ (orientation error to the path) will not be affected by this switching. The same occurs for the human orientation with respect to robot ψ_H which is always controlled by the human. Thus, these states are globally uniformly asymptotically stable (GUAS) with respect to the switching signal within the interaction zone. Now, when the human exits the interaction zone and the robot stops, d value (robot to path distance) remains fixed, and only globally uniformly stability (GUS) can be proved. Next, the switching effect over $\tilde{\rho}$ will be determined, considering that this error is alternatively controlled by the robot and by the human.

Table 1 Relation and σ_A velocities with zones

σ_A	***Human in the Zone***	***Velocity***
0	*1H or 2H*	$any v_H$
1	*1R or 2R*	$v_H \geq v_{Rmax}$
2	*1R*	$v_{Rmin} < v_H < v_{Rmax}$
3	*2R*	$v_{Rmin} < v_H < v_{Rmax}$

Figure 13 shows most compromising cases for the switching system stability: in Fig. 13a when the human passes from *Zone 1R* to*Zone 1H* with $v_H < v_{Rmin}$ and then in Fig. 13b when the human passes from *Zone 1H* to *Zone 1R* with $v_H > v_{Rmax}$. It can also be concluded that this delay avoids chattering, since it acts as an hysteresis for this switching. With reference to Fig. 13 in $[t_k t_{k+1}]$ operates the human, noting an increasing of $\tilde{\rho}(t)$ related to the human reaction time to control this distance, and then an asymptotic behavior of $\tilde{\rho}(t)$ to zero when the human controls $\tilde{\rho}\,(t)$ after the time delay (dashed line). In the interval $[t_{k+1} t_{k+2}]$ it operates the robot and

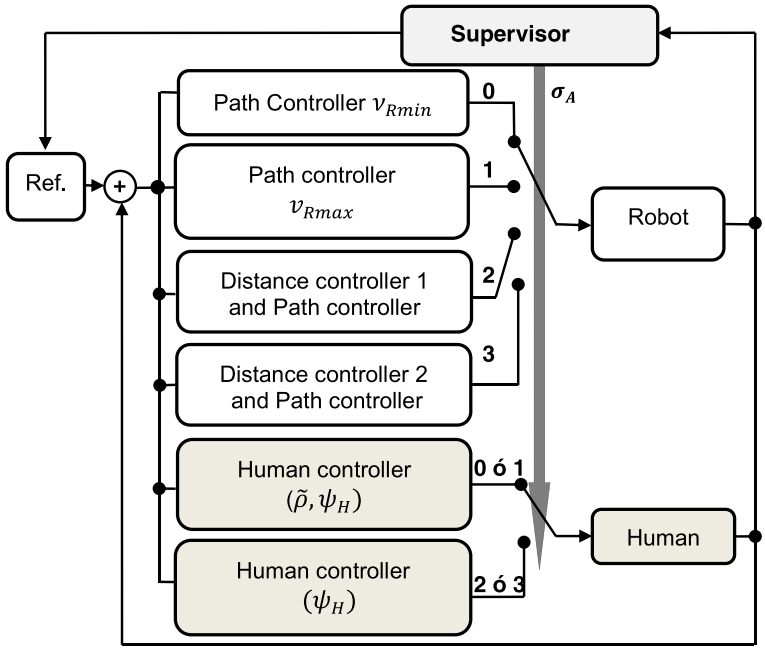

Fig. 12 Switched system block diagram

$\tilde{\rho}(t)$ decreases. By considering the kinematics of this problem (2), a distance error $\tilde{\rho}_\tau$ can be defined during τ as a function of the human and robot velocities:

$$\tilde{\rho}_\tau = \tau\,(v_H \cos\psi_H - v_R \cos\psi_R) \tag{26}$$

This distance directly depends on the relative human to robot velocity and presents two extreme cases: the first one when $v_H < v_{Rmin}$ and hence $v_R = v_{Rmin}$ (Fig. 13.a), while that in Fig. 13.b appears for $v_H > v_{Rmax}$ and hence $v_R = v_{Rmax}$. In both cases these relative velocities act only up to $t = \tau$ since after this time interval, the human or the robot corrects the error. The following analysis is for the most critical case when the human doesn't control $\tilde{\rho}$ after delay τ (Fig. 13.c). Then, when the *human controller* ($k_j = k_H$)or the robot controller($k_j = k_R$) are active, the evolution of $\tilde{\rho}(t)$ will decay exponentially to zero. However, during the pure delay, lineal growth will be supposed according to:

$$\begin{aligned} &\frac{\tilde{\rho}_\tau}{(}t - t_k);\ t_k < t \le t_{k+1} \\ &\tilde{\rho}_\tau e^{-k_j}(t - t_k - \tau);\ t_{k+1} \le t < t_{k+2} \end{aligned} \tag{27}$$

A correction time of at least t_c seconds is necessary in order to guarantee stability. Therefore, the objective is to compute the minimum time t_c that the robot controller needs to be active in order to correct the error due to the human delay. From

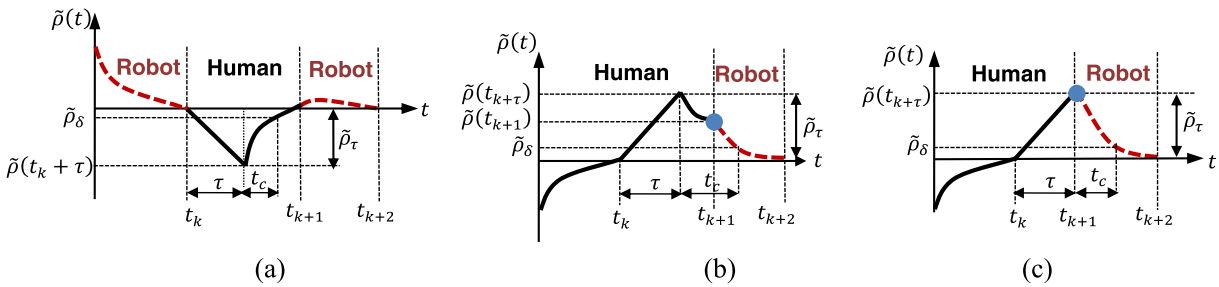

Fig. 13 Switching system: solid black when human controls and dashed red when the robot is controlling $\tilde{\rho}$.**(a)** Switching from*Zone 1H* to*Zone 1H* with $v_H < v_{Rmin}$. **(b)** Switching from*Zone 1H* to*Zone 1R* with $v_H > v_{Rmax}$blue circle indicates the instant at which $v_H = v_{Rmax}$. **(c)** Is the critic case(*b*)when the human don't control the $\tilde{\rho}$*after delay*

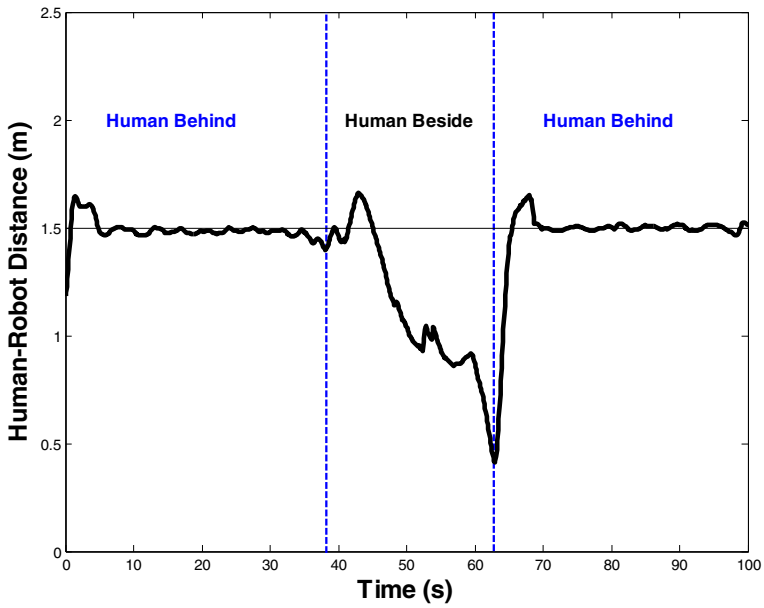

Fig. 14 Human location and human-robot distance experimental curves d_H

Fig. 13.c, the stability condition is $\tilde{\rho}_\tau e^{-k_j t_c} < \tilde{\rho}_\delta$ with $t = t_k + \tau + t_c$; where $\tilde{\rho}_\delta$is the maximum error in order to consider that the properly corrected error. Then, it is possible to compute the minimum time required to compensate the error due to the human delay:

$$t_c > -\left(\frac{1}{k_j}\right)\log\left(\frac{\tilde{\rho}_\delta}{\tilde{\rho}_\tau}\right) \tag{28}$$

Expression (28) represents the minimum time that robot has to maintain its controller active before making a new switching (i.e., before delegating the distance regulation to the human again).

4.2 Stability Analysis of Human-Robot Switching: Lateral-Human Location

Analogously to Section IV.A, it can be noted that the control states for the human considered as a control plant are $\tilde{\rho}$ and ψ_H, whereas the control states for the robot are $\tilde{\rho}_x$ (lateral distance error), d and $\tilde{\psi}$. Also in this case ψ_H is corrected by the human for

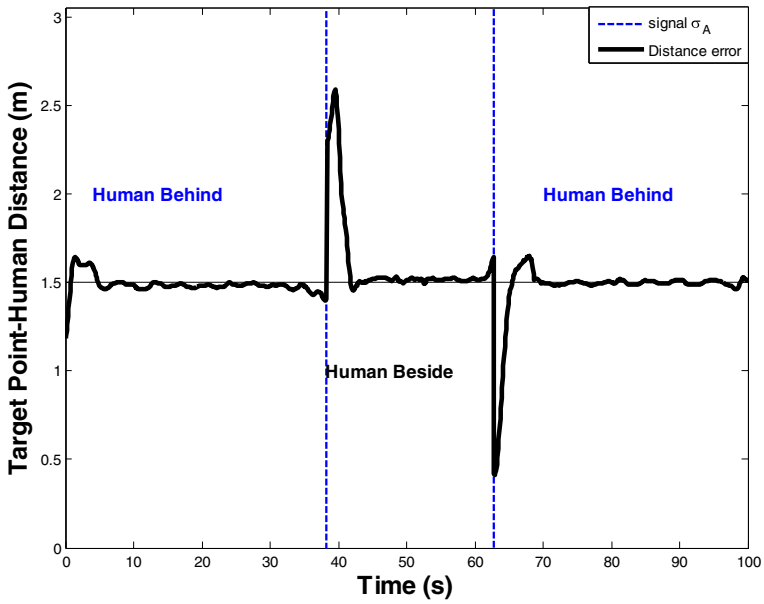

Fig. 15 Evolution of distance ρ and human location

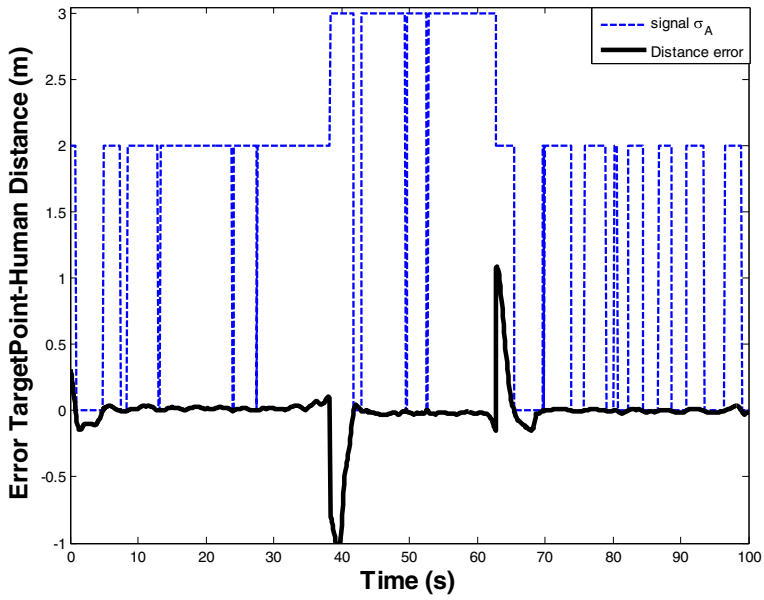

Fig. 16 Evolution of distance error $\tilde{\rho}$ and signal σ_A

any σ_A value. On the other hand it has been proved that $\tilde{\rho}$ is AS when the *human controller* is active at $\sigma_A = 0$ and $\sigma_A = 1$, whereas $\tilde{\rho}_x$ is AS when the robot is controlling at $\sigma_A = 3$. As in this case, there is a known relationship between them: $\tilde{\rho}^2 = \tilde{\rho}_x^2 + \tilde{\rho}_y^2$. Now, considering again the AS result for $\tilde{\rho}$ thus $\tilde{\rho}_x$ must be also an AS behavior. Finally, the switching system is stable if Eq. 28 is satisfied. The switching analysis over the control states for the path following controller is identical to the one presented before.

4.3 Stability Analysis of System: Human Besides/Behind Robot

To complete stability analysis it is mandatory to consider all cases at which the human alternates its position from behind to beside the robot, which are: *i*)

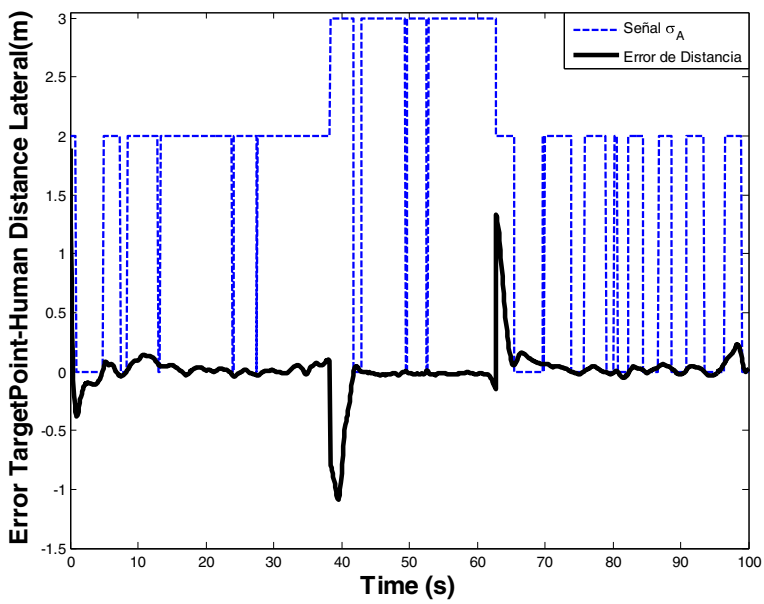

Fig. 17 Evolution of distance error $\tilde{\rho}_x$ and signal σ_A

the human passes from *Zone 1H* to *Zone 2H* and vice versa; *ii)* the human passes from *Zone 1R* to *Zone 2H* and vice versa. In case *i*) the human controls $\tilde{\rho}$ and ψ_H in both zones whereas the robot is moving at minimum velocity over the path. Hence, this change on the human zone does not affect robot stability. In case *ii)* when the human is in *Zone 1R* and decides to go to *Zone 2H* the robot changes its velocity to the minimum velocity and from this moment $\tilde{\rho}$ is controlled by the human. While the human is in Zone 2H and decides to go to *Zone 1R* and from this moment on, $\tilde{\rho}$ is controlled by the robot and if Eqs. 4 and 28 is fulfilled $\tilde{\rho}$ es AS.

5 Experimental Results

In order to validate the controllers, experiments have been performed with a Pioneer 3AT mobile robot and a LMS200 laser range finder (180° range with 1° resolution) along with a leg detection algorithm developed to measure the variables of interest (distance, position, orientation and velocity). Constants of the robot controllers are set to the following values: $k_{satx} = 0.5$; $k_{saty} = 0.5$; $k_x = 0.95$; $k_y = 0.95$; $k_{sat\rho} = 0.9$, $k_\rho = 1.5$; $k_{satL\rho} = 3$ and $k_{L\rho} = 1.8$. Person who participated in the experiment is a 30 years old man. Only consideration in the person selection were that he/she must be capable to walk at a minimum speed above v_{Rmin}. To validate the switched control system, two experiments are shown. In the first experiment the robot follows a circular path and the person was asked to start follow the robot from behind. He was also asked to change his relative position to the robot from behind to beside it and return behind the robot at any time he wants. No specification about the walking speed was given to the man. Therefore, initially the human is located behind the robot. The human starts following the robot behind it with $\rho_d = 1.5m$ then he decides at $t = 39s$ to walk beside the robot and finally at $t = 62s$ the man returns behind the robot. Figure 14 shows the location of the human during all interaction and human-robot distance experimental curve d_H. Note that when the human is located behind the robot $d_H = \rho$, while, when the human is located beside the robot, the robot can't control $\tilde{\rho}_y$ and $d_H \neq \rho$.

Figure 15 shows distance experimental curve ρ and the location of the human during all interaction, the curve ρ converges to $\rho_d = 1.5$m. Note that, the distance ρ presents jumps at $t = 39s$ and $t = 62s$, this is due to changes in target point position. The maximum amplitude of these jumps is given by $\rho_{max} - \rho_d or \rho_d - \rho_{min}$, in this case is $1.1m$ with $\rho_{min} = 0.4m$ and $\rho_{max} = 2m$.

Figure 16 shows the time evolution of the distance $\tilde{\rho}$ with the switching signal σ_A. while Fig. 17 shows

Fig. 18 Second experiment sequence: robot leading the human through a corridor

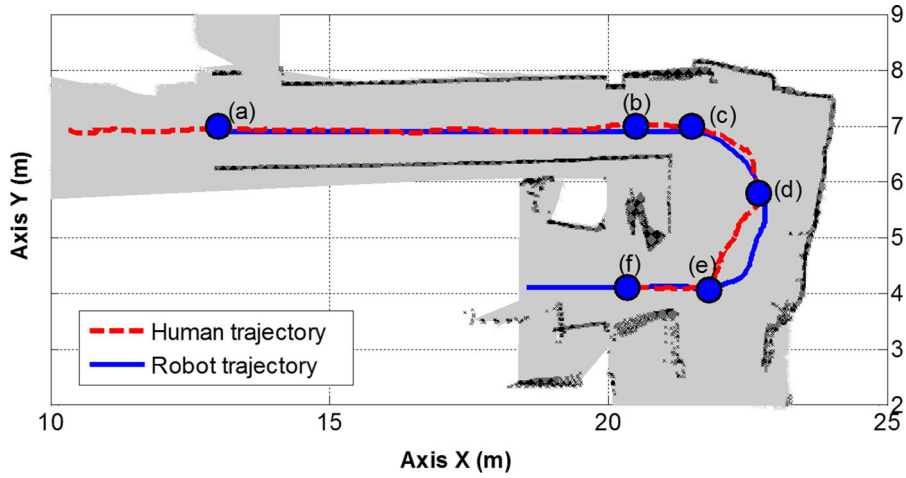

Fig. 19 Human and robot Trajectories

the time evolution of the distance $\tilde{\rho}_x$ with the switching signal σ_A. The distance controller 1 (behind) is active ($\sigma_A = 2$, i.e., the human walks behind the robot) between $t = 0s$ and $t = 38s$, and between $t = 63s$ and $t = 100s$. On the other hand, the distance controller 2 (beside) is active ($\sigma_A = 3$, i.e., the human walks beside the robot) between $t = 39s$ and $t = 62s$. Note in Fig. 16 that the state $\tilde{\rho}_x$ only is controlled when the human decides to walk beside the robot.

In the second experiment the robot guides the human being along one corridor until the desired final position inside the library, with $\rho_d = 1.5m$. For this experiment the same 30 years old man was asked to follow the robot without any specification about the relative position (behind or beside) or about the walking speed. He was also asked to stop following the robot for a few seconds at any instant he wants. This action would simulate that the human has not the intension of interact with the robot, allowing evaluate the robot performance under this situation. During the experiment, the human decided to follow the robot always from behind may be because of the reduced wide of the corridor. In this experiment, the human always walked behind the robot.

Figure 18 reveals a photogram sequence of the experiment. Figure 19 depicts the described trajectory. Figure 20 shows the time evolution of the human-target point distance (in this case the target point is

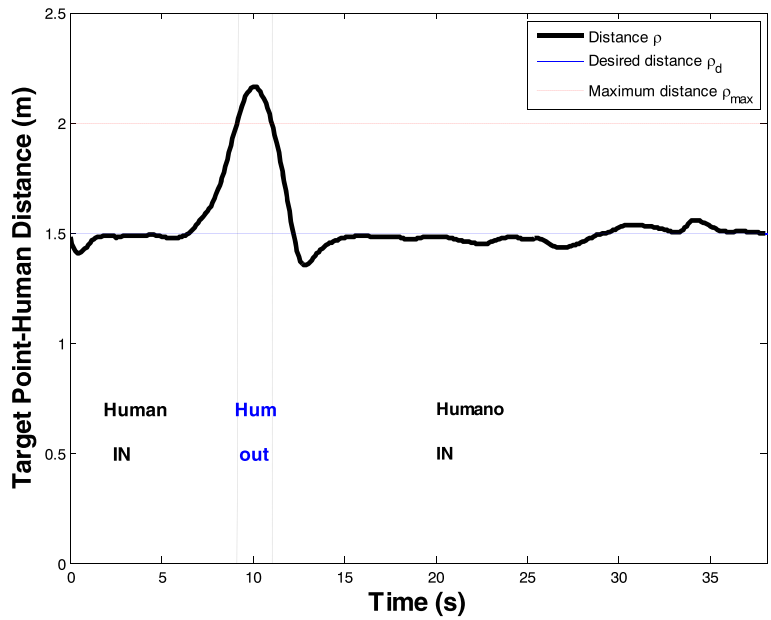

Fig. 20 human location vs. distance experimental curves ρ

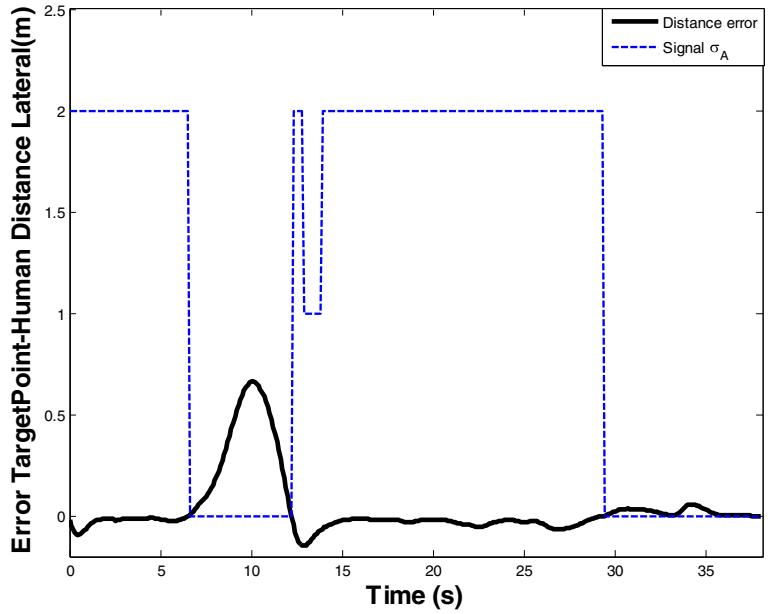

Fig. 21 human location vs. error distance experimental curves $\tilde{\rho}$

on the robot). Note that at $t = 7s$ the human stops (Fig. 21) making the distance increase (human exits the interaction zone), delegating the responsibility of controlling the distance to the human since the robot cannot go back. When the human exceed the robot maximum speed, the robot takes a $v_{Rmax} = 0.75m/s$ as shows Fig. 22 at $t = 13s$ ($\sigma_A = 1$). From $t = 14s$ the robot takes control of the distance until it achieves the desired final position. Distance errors less than $7cm$ are observed.

Figures 16 and 21 verified that the time intervals in which the robot is active exceed the value of $t_c = 0.25s$, which is the minimum time before the control will switch back to the human. The time was calculated from Eq. 24 for critical conditions where $k_R = 8.8$, $\tilde{\rho}_\delta = 0.07m$ being the most critical case

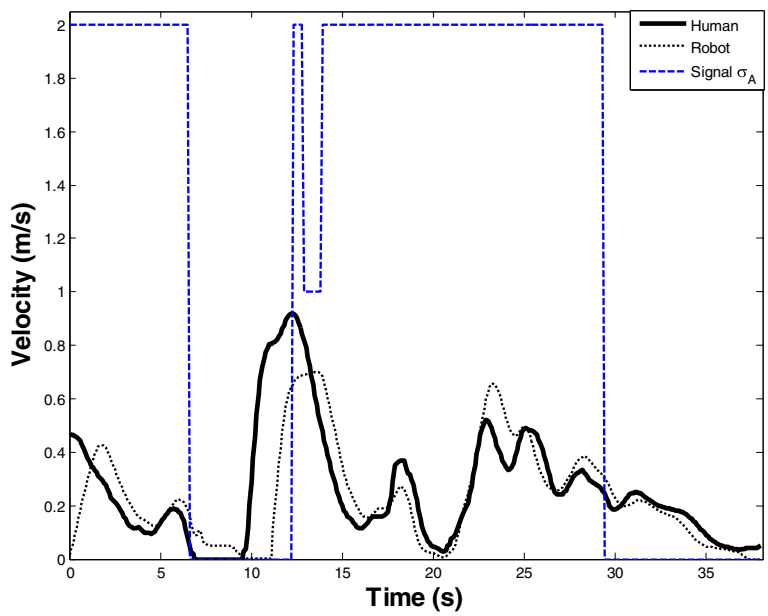

Fig. 22 Velocity and human to robot distance with switching signal

when v_H and v_R are collinear ($\psi_H = \psi_R = 0$) then $\tilde{\rho}_\tau = 0.675m$, $v_H = 2v_{Rmax}$.

Figures 16 and 21 verified that the time intervals in which the robot is active exceed the $t_c = 0.25s$, it is the minimum time before the control will switch back to the human. The time was calculated from Eq. **??** for critical conditions where $k_R = 8.8$, $\tilde{\rho}_\delta = 0.07m$, the most critical case when v_H and v_R are collinear ($\psi_H = \psi_R = 0$) then $\tilde{\rho}_\tau = 0.675m$, $v_H = 2v_{Rmax}$.

6 Conclusions

This work has presented the development and analysis of a bilateral interaction system between a human being and a robot. The robot has to guide the person while it follows a specified path. The proposed interaction control system is said to be bilateral because it considers the active participation of the human and the robot in the control problem. To emphasize this interaction the human has no passive attitude with respect to the robot, but he can take control of some system objectives in certain situations. A nonlinear kinematic controller for modelling the human being behaviour in the considered task has also been proposed and validated. Experimental results show the good performance of the proposed control algorithms in the bilateral human-robot interaction for the considered problem. It has been found through experiments that the robot must comply a minimum activation time for the system to be stable. It is important to highlight that the work includes the theoretical stability proof not only for the independent control algorithms but also for the complete switched system proposed. Future research work is expected to implement dynamic interaction zones in scenarios with multiple humans and multiple robots.

References

1. Capi, G., Toda, H., Nagasaki, T.: A vision based robot navigation and human tracking for social robotics. IEEE Int. Work. Robot. Sens. Environ. **22**, 1–6 (2010)
2. Bellotto, N., Huosheng, H.: Multisensor-based human detection and tracking for mobile service robots. IEEE Trans. Syst. Man, Cybernet. **39**, 167–181 (2009)
3. Sisbot, E.A., Marin, L.F., Alami, R., Simeon, T.: A Human Aware Mobile Robot Motion Planner. IEEE Trans. Robot. **23**, 874–883 (2007)
4. Garrell, A., Sanfeliu, A.: Local optimization of cooperative robot movements for guiding and regrouping people in a guiding mission. IEEE/RSJ International Conference on Intelligent Robot and System (IROS). pp. 3294–3299 (2010)
5. Lam, C.P., Chou, C.T., Chiang, K.H., Fu, L.C.: Human-centered robot navigation-now a harmoniously human-robot coexisting environment. IEEE Trans. Robot. **27**, 1873–1818 (2011)
6. Shiomi, M., Kanda, T., Ishiguro, H., Hagita, N.: Interactive humanoid robots for a science museum. IEEE Intell. Syst. **22**, 25–32 (2007)
7. Faber, F., et al.: The humanoid museum tour guide Robotinho. The 18th IEEE International Symposium on Robot and Human Interactive Communication. pp. 891–896 (2009)
8. Kim, H., Chung, W., Yoo, Y.: Detection and tracking of human legs for a mobile service robot. IEEE/ASME International Conference on Advanced Intelligent Mechatronics. pp. 812–817 (2010)
9. MacRuer, D.T., Jex, H.R.: A Review of Quasi-Linear Pilot Models. IEEE Trans. Human Factors Electron. **8**, 231–248 (1967)
10. Lee, K.K., Yu, M., Xu, Y.: Modeling of human walking trajectories for surveillance. IEEE/RSJ Int. Conf. Intell. Robot. Syst. **2**, 1554–1559 (2003)
11. Alvarez, A., Trivino, G., Cordon, O.: Human gait modeling using a genetic fuzzy finite state machine. IEEE Trans. Fuzzy Syst. **20**, 205–223 (2012)
12. Awang, S., Shamsuddin, S.M.: 3D Human movement (walking) modeling using neural network. IEEE International Conference on Computing & informatics. pp. 1–4 (2006)
13. Arechavaleta, G., Laumond, J.P., Hicheur, H., Berthoz, A.: The no-holonomic nature of human locomotion: a modeling study. The first IEEE/RAS-EMBS International Conference on Biomedical Robotics and Biomechatronics. pp. 158–163 (2010)
14. Slawiñski, E., Postigo, J., Mut, V.: Stable teleoperation of mobile robots. Proceedings IEEE International Conference on Mechatronics and Automation. pp. 318–323 (2006)
15. Wang, Q., Wei, K., Wang, L., D. L.: Modeling and stability analysis of human normal walking with implications for the evolution of the foot. 3rd IEEE RAS & EMB International Conference on Biomedical Robotics and Biomechatronics. pp. 479–484 (2010)
16. Sreenivasa, M., Soueres, P., Laumond, J.: Walking to grasp: modeling of human movements as invariants and an application. IEEE Trans. Syst. Man Cybern. **42**, 880–893 (2012)
17. Andaluz, V., Roberti, F., Toibero, J.M., Carelli, R., Wagner, B.: Adaptive Dynamic Path Following Control of an Unicycle-Like Mobile Robot. In: Jeschke, S., Liu, H., Schilberg, D. (eds.): Lecture Notes in Computer Science: Intelligent Robotics and Applications, pp. 563–574. Berlin Heidelberg. Springer-Verlag (2011)
18. Arechavaleta, G., Laumond, J.P., Hicheur, H., Berthoz, A.: An Optimality Principle Governing Human Walking. IEEE Trans. Robot. **24**(1), 5–14 (2008)

19. Hicheur, H., Pham, Q.C., Arechavaleta, G., Laumond, J.P., Berthoz, A.: The formation of trajectories during goal-oriented locomotion in humans. I. A stereotyped behavior. Eur. J. Neurosci. **26**, 2376–2390 (2007)
20. Pham, Q.C., Hicheur, H., Arechavaleta, G., Laumond, J.P., Berthoz, A.: The formation of trajectories during goal-oriented locomotion in humans. II. A maximum smoothness model. Eur. J. Neurosci. **26**, 2391–2403 (2007)
21. Silviu-lulian, N.: Delay effects on stability a robust control Approach. Chapter 3 (pp. 107-111) and chapter 5 (pp. 198-205). Springer, London (2001)
22. Toibero, J.M., Roberti, F., Carelli, R., Fiorini, P.: Switching control approach for stable navigation of mobile robots in unknown environments. Robot. Comput. Integr. Manuf. **27**, 558–568 (2011)
23. Linh, V., Morgansen, K.A.: Stability of Time-Delay Feedback Switched Linear Systems. IEEE Trans. Autom. Control **55**(10), 2385–2390 (2010)
24. Chen, W.H., Zheng, W.X.: Delay-independent minimum dwell time for exponential stability of uncertain switched delay systems. IEEE Trans. Autom. Control **55**(10), 2406–2413 (2010)
25. Caliskan, S.Y., Ozbay, H., Niculescu, S.I.: Dwell-time computation for stability of switched systems with time delays. IET Control Theory & Appl. **7**(10), 1422–1428 (2013)
26. Sun, Z., Ge, S.S.: Stability Theory of Switched Dynamical Systems. Springer Verlag London Limited (2011)